ACS APPLIED MATERIALS & INTERFACES

Research Article

www.acsami.org

Laundering Durability of Photocatalyzed Self-Cleaning Cotton Fabric with TiO_2 Nanoparticles Covalently Immobilized

Ming Yu,[†,‡] Ziqiang Wang,[†,‡] Hanzhou Liu,[‡,§] Siyuan Xie,[‡,§] Jingxia Wu,[‡,§] Haiqing Jiang,[‡] Jianyong Zhang,[‡] Linfan Li,[‡] and Jingye Li*[,‡]

[‡]TMSR Research Center and CAS Key Lab of Nuclear Radiation and Nuclear Energy Technology, Shanghai Institute of Applied Physics, Chinese Academy of Sciences, Shanghai 201800, P. R. China

[§]University of Chinese Academy of Sciences, Beijing 100049, P. R. China

Supporting Information

ABSTRACT: Photocatalyzed self-cleaning cotton fabrics with TiO_2 nanoparticles covalently immobilized are obtained by cograft polymerization of 2-hydroxyethyl acrylate (HEA) together with the surface functionalized TiO_2 nanoparticles under γ-ray irradiation. The covalent bonds between the TiO_2 nanoparticles and cotton fabrics bridged by poly(2-hydroxyethyl acrylate) (PHEA) graft chains is strong enough to survive 30 accelerated laundering circles, equivalent to 150 commercial or domestic launderings.

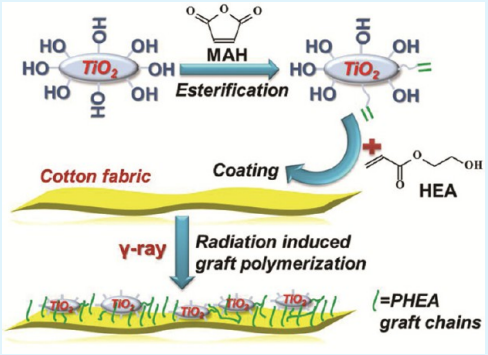

KEYWORDS: *laundering durability, self-cleaning, TiO_2 nanoparticles, radiation induced graft polymerization*

INTRODUCTION

Self-cleaning materials have received much attention lately for their obvious advantages in industry and daily life. There are two routes to preparation of self-cleaning materials. One is to prepare a superhydrophobic surface[1−6] with low surface energy chemical structures combined with microstructural roughness where dirt is removed by water droplets that roll across the surface, which is well-known as the "lotus effect".[7−12] The other route is to prepare a hydrophilic surface containing a photocatalyst on which water-soluble dirt is easily washed off and the organic pollutants on the surface are removed by photocatalyzed degradation under ultraviolet (UV) irradiation.[13−17] Very recently there have been reports of materials functionalized with both superhydrophobic and photocatalysis properties.[18] Since the adhesion of oily dirt may decrease the water-repellent properties of the superhydrophobic materials,[19] self-cleaning materials containing a photocatalyst may be more suitable for some practical applications, such as self-cleaning fabrics and clothes.

TiO_2 is one of the most commonly used photocatalysts[20−22] and has been widely employed in applications for wastewater treatment,[23,24] water splitting,[25] air purification,[26] chemical synthesis,[27] and electrode fabrication.[28,29] In recent years, there has been growing research interest in the preparation of self-cleaning fabrics thru the immobilization of TiO_2 nanoparticles on fabric surfaces via a coating method,[30,31] sol−gel method,[32,33] and surface-modification method by introducing a hydroxyl or carboxyl group onto the surface of the fabric to adsorb TiO_2 nanoparticles by charge effect.[34] In these self-cleaning fabrics, however, the binding force between TiO_2 nanoparticles and the fabric is quite weak and the usage durability needed for self-cleaning fabrics has been largely ignored.

In our previous work, a radiation-induced graft-polymerization technique was used to prepare a durable superhydrophobic cotton fabric for laundering, where covalent bonds enhance the binding force between cotton and low-surface-energy compounds.[35,36] However, it is much more difficult to form tight covalent bonding between TiO_2 nanoparticles and cotton fabrics. C═C bonds can be introduced onto the surface of TiO_2 nanoparticles by reaction with a vinyl monomer such as maleic anhydride (MAH) or acrylic acid, and the functionalized TiO_2 nanoparticles can be regarded as nanosize "giant" monomers. But the surface for the photocatalysis reaction should not be blocked by the surface organic functional groups, thus the density of C═C bonds on TiO_2 nanoparticles will not be high. Therefore, it is difficult to form an adequate amount of covalent bonds between functionalized TiO_2 nanoparticles and the cotton fabric, as the interface area is limited between them.

Here we utilize a new strategy to immobilize TiO_2 nanoparticles covalently onto a cotton fabric surface using a

Received: January 23, 2013
Accepted: April 12, 2013
Published: April 12, 2013

   dx.doi.org/10.1021/am400304s | ACS Appl. Mater. Interfaces 2013, 5, 3697−3703

monomer to form a graft chain network that involves TiO_2 nanoparticles. First, C═C bonds were introduced onto the surface of TiO_2 nanoparticles by an esterification reaction between the hydroxyl group on the TiO_2 nanoparticle surface with MAH; second, the functionalized TiO_2 nanoparticles (denoted as TiO_2-*g*-MAH) and 2-hydroxyethyl acrylate (HEA) were cografted onto cotton fabric induced by γ-ray irradiation (Scheme 1). The functionalized cotton fabrics (denoted as cotton-*g*-TiO_2) show a photocatalyzed self-cleaning property, and the covalent bonds between TiO_2 nanoparticles and cotton fabrics bridged by the poly(2-hydroxyethyl acrylate) (PHEA) graft chains are strong enough to survive an accelerated laundering durability test.

Scheme 1. Procedure of Covalent Immobilization of TiO_2 Nanoparticles onto Cotton Fabric

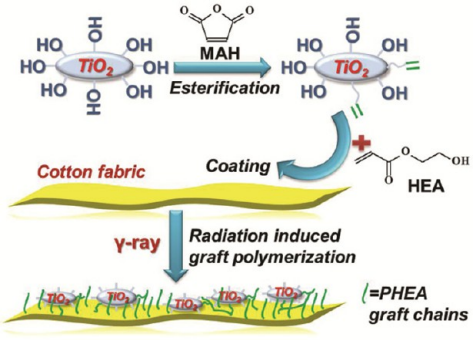

EXPERIMENTAL SECTION

Materials. TiO_2 nanoparticles with a purity of 99.8% and particle size from 5 to 10 nm, maleic anhydride (MAH) and anhydrous sodium acetate of analytical grade were purchased form Aladdin Industrial Inc. 2-Hydroxyethyl Acrylate (HEA) with a purity of 96% was purchased from Tokyo Chemical Industry Co., Ltd. Xylene, ethanol and acetone were all analytical grade and purchased from Sinopharm Chemical Reagent Co., Ltd. All these materials were used without further purification.

Modification of TiO_2 Nanoparticles. Thirty grams of TiO_2 nanoparticles, 40 g of MAH, and 0.1 g of anhydrous sodium acetate were added into 300 mL of dimethyl benzene. After 5 min of high shearing at 35 000 rpm, the mixture was heated to 140 °C. The esterification reaction lasted for 24 h, and then the modified nanoparticles was centrifugally separated and ultrasonically washed by acetone for five times.

Radiation-Induced Cograft Polymerization of HEA and TiO_2-*g*-MAH. Ethanol solutions with 20% (v./v.) HEA, were added with weighted TiO_2-*g*-MAH nanoparticles to prepare the dispersions with TiO_2-*g*-MAH concentration of 0, 5, 15, 25, and 35 g/L, respectively. The dispersions were well mixed by ultrasonication and then were padded to cotton fabric samples. After that, the cotton fabric samples were put into tubes and purged with nitrogen for 15 min to remove oxygen. The tubes were sealed and then irradiated by γ-ray in a ^{60}Co source for the absorbed dose of 30 kGy. Then the fabrics were extracted by ethanol for 72 h in a Soxhlet apparatus to remove any residual monomer, homopolymer, and nanoparticles. Finally, the modified cotton fabrics were vacuum-dried for further measurements.

Measurements. Fourier transform infrared (FT-IR) spectra were taken on a BRUKER TENSOR 27 FT-IR spectrometer. The TiO_2 and TiO_2-*g*-MAH nanoparticles were pressed into pellet with KBr. The pristine and functionalized cotton fabrics were measured under attenuated total reflection (ATR) method.

X-ray diffraction (XRD) analysis was performed on a RIGAKU D/Max2200 XRD instrument equipped with Cu−Kα radiation (λ = 1.54 Å).

Thermogravimetry analysis (TGA) was performed on a TG 209 F3 Tarsus (NETZSCH, Germany) instrument. The samples were heated from 50 to 700 °C at a heating rate of 10 °C/min under nitrogen atmosphere.

Contact angle (CA) analysis was performed on a KSV INSTITUTION (Attention Company) instrument and the volume of the water drop is 3 μL. Each sample was measured for three times on different positions and the average value was obtained.

Scanning electron microscopy (SEM) analysis was performed on a JEOL JSM-6700F SEM instrument. The pristine cotton fabric and functionalized cotton fabrics were deposited of gold by sputtering. The SEM voltage was set at 10 kV.

Transmission electron microscopy (TEM) analysis was performed on a FEI TECNAI G2 TEM instrument. The pristine TiO_2 nanoparticles and TiO_2-*g*-MAH were dispersed in ethanol by ultrasonication and dropped on copper net and vacuum-dried before analysis. The TEM voltage was set at 200 kV.

Photocatalyzed Self-Cleaning Effect Test. Oleic acid dyed with 5 g/L Oil Red was used as a model stain and dropped onto the cotton fabrics. The fabrics were then irradiated by UV with a wavelength of 355 nm under a light intensity of 2.0 ± 0.1 mW/cm^2 at specific time intervals.

Laundering Durability Test. A laundering durability evaluation was carried out according to AATCC (American Association of Textile Chemists and Colorists) Test method 61−2006, condition 2A. The cotton fabrics were cut into 50 mm × 150 mm patches and washed in a rotating closed canister containing 150 mL aqueous solution of an AATCC standard WOB detergent (0.15%, w/w) and 50 stainless steel balls in a thermostatically controlled water bath at 49 °C, 40 ± 2 rpm.

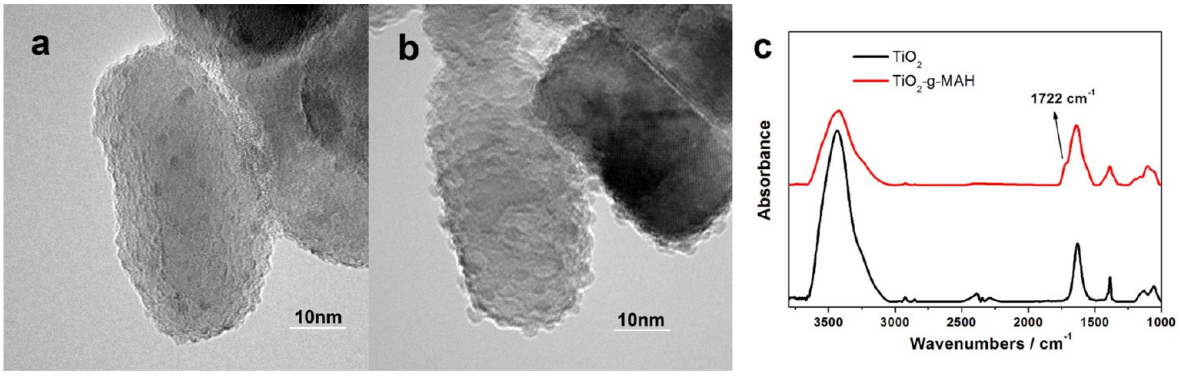

Figure 1. TEM images of (a) the pristine TiO_2 nanoparticles and (b) the TiO_2-*g*-MAH nanoparticles, and (c) the FT-IR spectra of the pristine TiO_2 and the TiO_2-*g*-MAH nanoparticles.

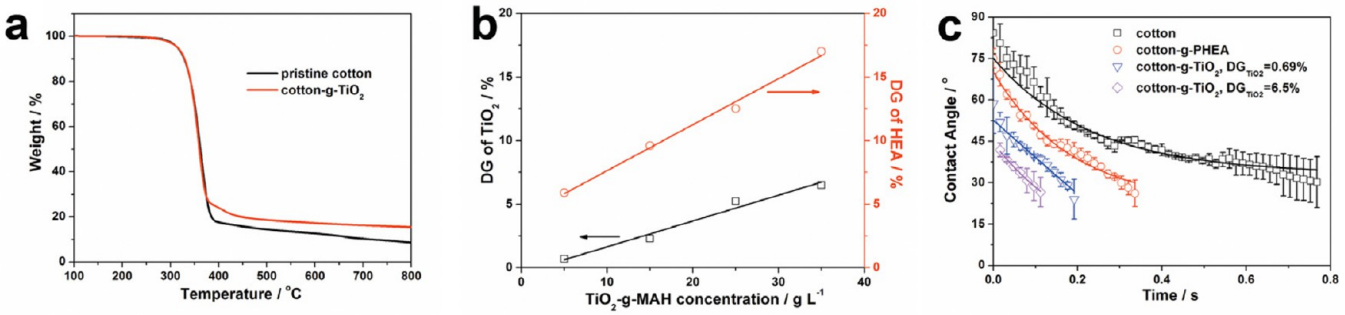

Figure 2. (a) TGA curves of the pristine cotton fabric and the cotton-*g*-TiO_2; (b) dependence of the DG of TiO_2-*g*-MAH nanoparticles and the DG of HEA graft chains on the amount of TiO_2-*g*-MAH nanoparticles immobilized; (c) CA of the pristine cotton fabric, the cotton-*g*-PHEA with DG_{HEA}= 6.9%, the cotton-*g*-TiO_2 with with DG_{HEA}= 5.9% and DG_{TiO_2} = 0.69%, and the cotton-*g*-TiO_2 with DG_{HEA}= 17.0% and DG_{TiO_2} = 6.5%.

Figure 3. SEM images of (a) the pristine cotton fabric (×300) and (b, c) the cotton-*g*-TiO_2 with DG_{HEA}= 17.0% and DG_{TiO_2} = 6.5% (b, ×300; c, ×50 000).

RESULTS AND DISCUSSION

The TiO_2 nanoparticles used in this research are in an anatase form, which has many hydroxyl groups on the surface and can react with other groups.[37] An esterification reaction between TiO_2 nanoparticles and MAH was carried out in dimethyl benzene and catalyzed by anhydrous sodium acetate. After the esterification reaction, some spherical domains appeared on the surface of the TiO_2 nanoparticles in the TEM images (Figure 1a, b) ascribed to the maleic acid group that was introduced. The success in the esterification is also confirmed by means of FT-IR spectra of the pristine TiO_2 and TiO_2-*g*-MAH (Figure 1c), where a new band at 1722 cm^{-1} due to the stretching vibration of carbonyl group in the FT-IR spectrum of TiO_2-*g*-MAH confirms the presence of maleic acid group on the surface of the TiO_2 nanoparticles. The content of the maleic acid esterified on the TiO_2-*g*-MAH nanoparticles was 2.7%, which was calculated from the TGA curves (see the Supporting Information, Figure S1). According to the DG of MAH, the size (about 25 × 25 × 50 nm) and the density (3.8 g/cm^3) of TiO_2 nanoparticles and the thickness (about 1 nm) and the density (1.1 g/cm^3) of the maleic acid layer on the surface of the nanoparticles, it can be calculated that about 2% of the surface area of the TiO_2 nanoparticles was covered by maleic acid. The maleic acid group had not covered the whole surface of the TiO_2-*g*-MAH and photocatalysis reactions can still be carried out on the surface of the TiO_2 nanoparticles exposed to the air. Because the crystal structure represents a critical factor for the photocatalytic properties of TiO_2 nanoparticles, X-ray diffraction (XRD) was used to investigate and compare the crystal structure of the obtained TiO_2-*g*-MAH nanoparticles (Supporting Information, Figure S2). The diffraction peaks at 25.2, 37.8, 47.9, 54.0, and 62.6° on the pattern of the pristine TiO_2 nanoparticles are the typical signals seen for an anatase crystal structure.[38] The pattern of the TiO_2-*g*-MAH nanoparticles was almost the same as the pristine nanoparticles, which indicates that the surface esterification reaction did not

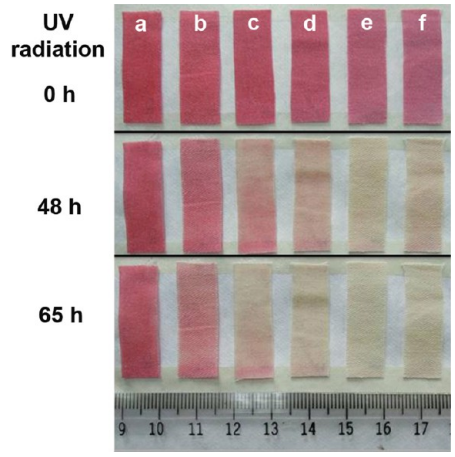

Figure 4. Photocatalyzed self-cleaning property of the functionalized cotton fabrics under the irradiation of UV light (355 nm, 2.0 ± 0.1 mW/cm^2). Oleic acid colored with 5 g/L oil red is used as model oil stain. The samples are (a) pristine cotton fabric, (b) cotton-*g*-PHEA (DG_{HEA} = 6.9%), (c) cotton-*g*-TiO_2 (DG_{HEA} = 5.9% and DG_{TiO2} = 0.69%), (d) cotton-*g*-TiO_2 (DG_{HEA} = 9.6% and DG_{TiO_2} = 2.3%), (e) cotton-*g*-TiO_2 (DG_{HEA} = 12.5% and DG_{TiO_2} = 5.2%), and (f) cotton-*g*-TiO_2 (DG_{HEA} = 17.0% and DG_{TiO_2} = 6.5%).

dx.doi.org/10.1021/am400304s | ACS Appl. Mater. Interfaces 2013, 5, 3697−3703

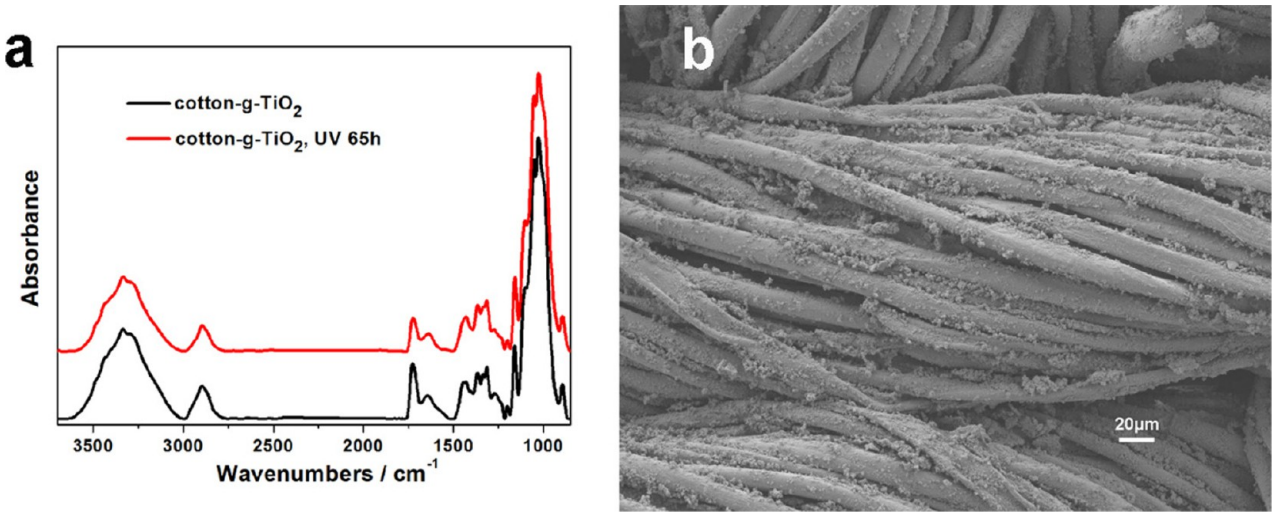

Figure 5. (a) FT-IR ATR spectra and (b) SEM images (×300) of cotton-*g*-TiO_2 fabric after UV (355 nm, 2.0 ± 0.1 mW/cm^2) irradiation for 65 h (DG_{HEA} = 17.0% and DG_{TiO2} = 6.5%).

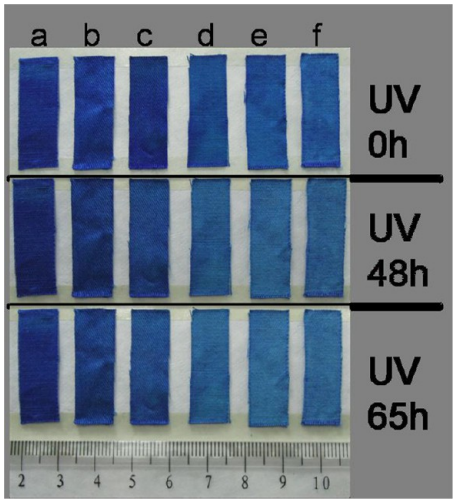

Figure 6. Dye stability test of the functionalized cotton fabrics under the irradiation of UV light (355 nm, 0.2 mW/cm^2). 2.5 g/L methylene blue aqueous solution is used as a dye. The samples are (a) pristine cotton fabric, (b) cotton-*g*-PHEA (DG_{HEA} = 6.9%), (c) cotton-*g*-TiO_2 (DG_{HEA} = 5.9% and DG_{TiO2} = 0.69%), (d) cotton-*g*-TiO_2 (DG_{HEA} = 9.6% and DG_{TiO2} = 2.3%), (e) cotton-*g*-TiO_2 (DG_{HEA} = 12.5% and DG_{TiO2} = 5.2%), and (f) cotton-g-TiO_2 (DG_{HEA} = 17.0% and DG_{TiO2} = 6.5%).

affect the crystal structure of the TiO_2 nanoparticles. The existing C═C bonds on the TiO_2-*g*-MAH nanoparticles, which is the reacting site for the following graft polymerization, was proven by the reaction with a Br_2 solution (see the Supporting Information, Figure S3), where the color of the Br_2 solution turned from yellow to colorless after the reaction, and the band at 395 nm due to Br_2[39] disappeared after the reaction in the UV−vis spectrum.

The TiO_2-*g*-MAH nanoparticles were immobilized onto the cotton fabric by cograft polymerization with HEA under *γ*-ray irradiation. After the graft polymerization, the cotton fabric was thoroughly washed and extracted to remove any residue homopolymers and unfixed TiO_2-*g*-MAH nanoparticles, and the functionalized cotton fabric was thus obtained. From the TGA curve (Figure 2a) of the cotton-*g*-TiO_2, there was obvious higher weight remaining after the degradation of most parts of the organic macromolecules, which should be attributed to the immobilized TiO_2 nanoparticles. Therefore, the DG of TiO_2 nanoparticles immobilized (denoted as DG_{TiO_2}) can be determined from the TGA curves, and the total DG can be calculated by the weight increase versus the original weight of the cotton fabric during the graft polymerization. Thus, the DG of grafted poly(2-hydroxyethyl acrylate) (denoted as DG_{HEA}) is the difference between DG and DG_{TiO_2}. In this work, the concentration of HEA used was fixed and the concentration of TiO_2-*g*-MAH nanoparticles was variable, and the dependence of the DGs on the concentration of TiO_2-*g*-MAH nanoparticles in the dispersions used is presented in Figure 2b. From the figure, it is obvious that both DG_{TiO2}, and also DG_{HEA} linearly increase with an increasing concentration of TiO_2-*g*-MAH nanoparticles. Here the TiO_2-*g*-MAH nanoparticles, that have many C═C bond arms, are both nanosize giant cross-linkers, and also the starting point for the graft polymerization under the *γ*-ray irradiation. That means that HEA was grafted onto both the cotton fabric and the coated TiO_2-*g*-MAH nanoparticles at the same time, and the PHEA graft chains form a network due to the cross-linking effect of TiO_2-*g*-MAH nanoparticles and thus the TiO_2 nanoparticles were covalently bonded to the cotton fibers.

Figure 2c shows the contact angles of the pristine cotton and the functionalized cotton fabrics with different DG_{TiO_2}. Although the cotton fabric is hydrophilic, the CA reduces with an increase in time and remains constant after 0.5 s at about 35°. As a comparison, HEA-grafted cotton fabric was prepared and tested, and the decreasing in CA is faster than the pristine sample due to the increased hydrophilicity from introduction of more hydroxyl bonds on the surface. Meanwhile, the functionalized cottons fabric shows dramatically faster reduction in CA, where the water drops spread out within 0.4 s. This is obviously due to the superhydrophilicity by the immobilized TiO_2 nanoparticles[40] and the surfaces of the TiO_2 nanoparticles are not fully covered by the grafted polymers, which is very important for the following photocatalyzing process.

The SEM images of the pristine cotton fabric and the functionalized cotton fabric are compared in Figures 3. From the image of the functionalized cotton fabric, the TiO_2

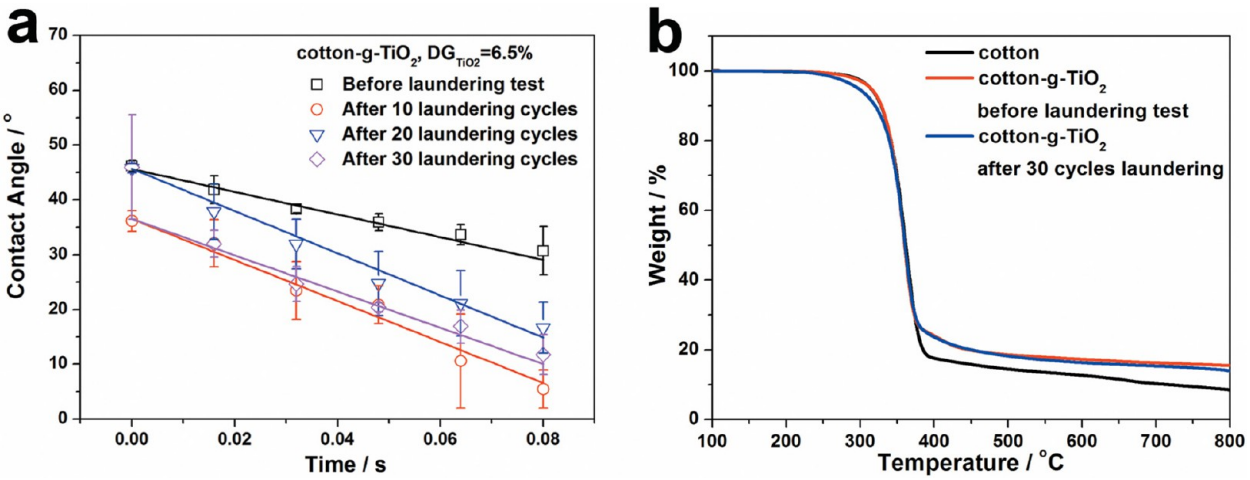

Figure 7. (a) CA of the cotton-*g*-TiO_2 (DG_{HEA} = 17.0% and DG_{TiO2} = 6.5%) before and after accelerated laundering test for 10, 20, and 30 cycles; (b) TGA curves of the pristine cotton fabric and the cotton-*g*-TiO_2 (DG_{HEA} = 17.0% and DG_{TiO2} = 6.5%) before and after accelerated laundering test for 30 cycles.

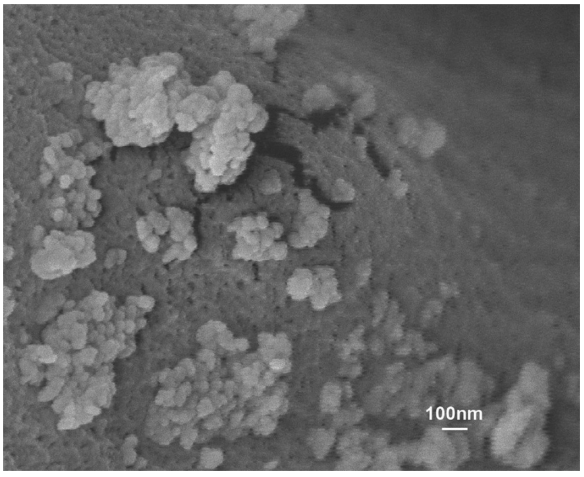

Figure 8. SEM images (×50 000) of the cotton-*g*-TiO_2 (DG_{HEA} = 17.0% and DG_{TiO_2} = 6.5%) after accelerated laundering test for 30 cycles.

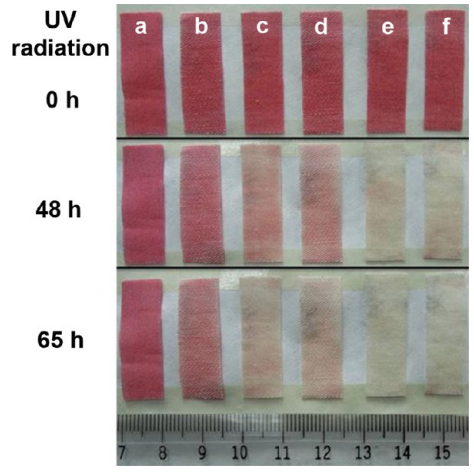

Figure 9. Photocatalyzed self-cleaning property of the fabrics after accelerated laundering test for 30 circles. Testing conditions are the same as those in Figure 3. The samples are (a) pristine cotton fabric, (b) cotton-*g*-PHEA (DG_{HEA} = 6.9%), (c) cotton-*g*-TiO_2 (DG_{HEA} = 5.9% and DG_{TiO2} = 0.69%), (d) cotton-*g*-TiO_2 (DG_{HEA} = 9.6% and DG_{TiO2} = 2.3%), (e) cotton-*g*-TiO_2 (DG_{HEA} = 12.5% and DG_{TiO2} = 5.2%), and (f) cotton-*g*-TiO_2 (DG_{HEA} = 17.0% and DG_{TiO2} = 6.5%).

nanoparticles are seen to be immobilized on the surface of the cotton fibers. From the amplified SEM image of the cotton-*g*-TiO_2 with DG_{TiO_2} = 6.5% (Figure 3c), the size of the TiO_2 nanoparticles immobilized on the surface of the cotton fibers is around 100 nm, which indicates that the nanoparticles are not severely aggregated.

Figure 4 presents the photocatalyzed self-cleaning effects of the functionalized cotton fabrics as compared with the pristine sample, and oleic acid dyed with Oil Red was used as a model organic stain. As expected, the pristine cotton fabric and the cotton-*g*-PHEA are still red in color no matter how long they are UV irradiated. In comparison, the red color disappeared on the cotton-*g*-TiO_2 under ultraviolet irradiation because of the photocatalyzed degradation of the oleic acid and Oil Red on the surface of TiO_2 nanoparticles.[41,42] Obviously, the high DG_{TiO_2}, which means that there are more TiO_2 nanoparticles covalently immobilized on the surface of the cotton fabric, the quicker the fabric bleached, due to the existence of more reaction sites for the photocatalyzed degradation of the organic stains. From the FT-IR ATR spectra of the cotton-*g*-TiO_2 fabric before and after UV irradiation (Figure 5a), it can be found that the intensity of the band due to the ester group[43] of the PHEA graft chain at 1720 cm^{-1} decreased a little, which indicated some of the PHEA graft chain were also degraded by the photocatalyzed reaction on the surface of TiO_2 nanoparticles. The band still has strong intensity, because the PHEA graft chain formed a network with the giant cross-linker, i.e., the TiO_2-*g*-MAH nanoparticles, during the cograft polymerization, there should be plenty of covalent bonds bridging the TiO_2 nanoparticles to the cotton fabric even after UV irradiation. The UV irradiation also has little effect on the morphology of the functionalized cotton fabric, which is confirmed by the SEM images (Figure 5b).

In contrast to the oil-soluble stains, when the cotton-*g*-TiO_2 fabrics were colored with a water-soluble dye such as methylene blue, it did not degrade under UV irradiation no matter how much the TiO_2 nanoparticles were immobilized (Figure 6), and does not show the same trend as in the previous reference.[44,45] The reason for this is the photocatalyzed degradation can take

place only when the pollutants are located in close vicinity to the TiO_2 nanoparticle surface[46] and the water-soluble methylene blue is absorbed by the numerous tiny pores in the cotton fibers, therefore it does not come into contact with the TiO_2 nanoparticles who are on the surface of the cotton fibers. To measure the color fastness of methylene blue on the cotton-*g*-TiO_2 fabric, a laundering durability evaluation was carried out according to AATCC (American Association of Textile Chemists and Colorists) Test Method 61−2006, condition 2A, where one accelerated laundering cycle equals five home or commercial launderings. The samples were cut into 50 mm × 150 mm patches and tested with a surfactant and stainless steel balls in warm water (see the Supporting Information, Figure S4). From the images of the laundered cotton-*g*-TiO_2 fabric (see the Supporting Information, Figure S5), it can be found the color became lighter with the increasing times of the laundering circles. These results indicated that the remove of water-soluble dyes only depends on the strength of the interactions between the dyes and cotton fabric, but irrelevant with the photocatalyzed degradation caused by the TiO_2 nanoparticles. This means that cotton-*g*-TiO_2 fabrics are both photocatalyzed self-cleaning, and colorable with water-soluble dyes, which is important for commercial applications.

The same laundering durability evaluation (AATCC Test Method 61−2006, condition 2A) was carried out to evaluate how strong the covalent bonds were between TiO_2 nanoparticles and cotton fabric bridged by PHEA graft chains. Because the spreading out of water droplets is faster on cotton-*g*-TiO_2 fabrics than on pristine cotton fabric or cotton-g-PHEA fabric, the CA valuation was used as a quick indicator of surface chemical changes after the laundering test. From Figure 7a, there was no obvious difference in the spreading speed of the water droplet on the cotton-*g*-TiO_2 fabric, which means the TiO_2 nanoparticles still exist on the surface of the fabric. The TGA curves tell the same story (Figure 7b), where the change in the remaining weight due to the TiO_2 nanoparticles was very small. From the SEM image (Figure 8) of the fabrics after 30 accelerated laundering tests, there were still many TiO_2 nanoparticles sticking on the surface of the fibers, just like mushrooms growing on a wall.

From the characterization, most of the TiO_2 nanoparticles were still immobilized on the surface of the cotton fibers after 30 accelerated laundering circles (which is equivalent to 150 instances of commercial or domestic launderings), because of the strengthening of covalent bonds between TiO_2 nanoparticles and cotton fabrics bridged by PHEA graft chains. Therefore, the photocatalyzed self-cleaning effect is retained after the laundering test, which was tested and presented in Figure 9. The image is almost the same as that in Figure 4, indicating that the photocatalyzed self-cleaning ability is unchanged after the accelerated laundering test thanks to the strengthened covalent bonds. This indicates that our strategy of forming covalent bonds between TiO_2 nanoparticles and cotton fabrics bridged by PHEA graft chains was quite successful.

CONCLUSIONS

TiO_2 nanoparticles were covalently immobilized onto cotton fabrics, first by esterification with MAH, and then cografting with HEA under γ-ray irradiation. The functionalized cotton fabrics, i.e. cotton-g-TiO_2 fabrics, show improved hydrophilicity as compared with pristine cotton fabric, and were enabled with a photocatalyzed self-cleaning effect under UV light radiation. An accelerated laundering durability experiment was conducted to measure the effects of the strength of the covalent bonds between the TiO_2 nanoparticles and cotton fabrics bridged by PHEA graft chains. From the characterization, most of the TiO_2 nanoparticles were still immobilized on the surface of the cotton fibers after 30 accelerated laundering circles (which is equivalent to 150 instances of commercial or domestic launderings), and therefore, the photocatalyzed self-cleaning ability of the functionalized cotton fabrics was well-retained.

ASSOCIATED CONTENT

Supporting Information

TGA curves of the pristine TiO_2 nanoparticles and the TiO_2-*g*-MAH nanoparticles. X-ray diffraction (XRD) spectra of the pristine TiO_2 nanoparticles and the TiO_2-*g*-MAH nanoparticles. Proving the existence of the carbon−carbon double bonds on the TiO_2-*g*-MAH nanoparticles including: (a) Images of Br_2 solution before and after reaction with the TiO_2-*g*-MAH nanoparticles. (b) UV−vis spectra of Br_2 solution before and after reaction with the TiO_2-*g*-MAH nanoparticles. Set-up of the accelerated laundering test according to AATCC Test method 61-2006 2A. Images of the functionalized cotton fabric colored by methylene blue after accelerated laundering and UV irradiation. This material is available free of charge via the Internet at http://pubs.acs.org.

AUTHOR INFORMATION

Corresponding Author

*E-mail: jingyeli@sinap.ac.cn.

Notes

The authors declare no competing financial interest.

†M.Y. and Z.W. are co-first authors.

ACKNOWLEDGMENTS

This work was supported by the National Natural Science Foundation of China (Grants 11175234 and 11105210), the "Strategic Priority Research Program" of the Chinese Academy of Sciences (Grant XDA02040300), the "Knowledge Innovation Program" of the Chinese Academy of Sciences (Grant KJCX2-YW-N49), and Shanghai Municipal Commission for Science and Technology (Grants 11ZR1445400 and 12ZR1453300).

REFERENCES

(1) Feng, L.; Li, S.; Li, Y.; Li, H.; Zhang, L.; Zhai, J.; Song, Y.; Liu, B.; Jiang, L.; Zhu, D. *Adv. Mater.* **2002**, *14*, 1857−1860.
(2) Frstner, R.; Barthlott, W.; Neinhuis, C.; Walzel, P. *Langmuir* **2005**, *21*, 956−961.
(3) Roach, P.; Shirtcliffe, N. J.; Newton, M. I. *Soft Matter* **2008**, *4*, 224−240.
(4) Wang, L.; Zhang, X.; Li, B.; Sun, P.; Yang, J.; Xu, H.; Liu, Y. *ACS Appl. Mater. Inter.* **2011**, *3*, 1277−1281.
(5) Ding, X.; Zhou, S.; Gu, G.; Wu, L. *J. Mater. Chem.* **2011**, *21*, 6161−6164.
(6) Li, L.; Breedveld, V.; Hess, D. W. *ACS Appl. Mater. Interfaces* **2012**, *4*, 4549−4556.
(7) Barthlott, W.; Neinhuis, C. *Planta* **1997**, *202*, 1−8.
(8) Blossey, R. *Nat. Mater.* **2003**, *2*, 301−306.
(9) Jiang, L.; Zhao, Y.; Zhai, J. *Angew. Chem., Int. Ed.* **2004**, *43*, 4338−4341.
(10) Marmur, A. *Langmuir* **2004**, *20*, 3517−3519.
(11) Nosonovsky, M.; Hejazi, V.; Nyong, A. E.; Rohatgi, P. K. *Langmuir* **2011**, *27*, 14419−14424.

(12) Yin, L.; Zhu, L.; Wang, Q.; Ding, J.; Chen, Q. *ACS Appl. Mater. Inter.* **2011**, *3*, 1254−1260.
(13) Parkin, I. P.; Palgrave, R. G. *J. Mater. Chem.* **2005**, *15*, 1689−1695.
(14) Guan, K. H. *Surf. Coat. Technol.* **2005**, *191*, 155−160.
(15) Xi, B.; Verma, L. K.; Li, J.; Bhatia, C. S.; Danner, A. J.; Yang, H.; Zeng, H. C. *ACS Appl. Mater. Inter.* **2012**, *4*, 1093−1102.
(16) Zhang, L.; Dillert, R.; Bahnemann, D.; Vormoor, M. *Energy Environ. Sci.* **2012**, *5*, 7491−7507.
(17) Anandan, S.; Rao, T. N.; Sathish, M.; Rangappa, D.; Honma, I.; Miyauchi, M. *ACS Appl. Mater. Inter.* **2013**, *5*, 207−212.
(18) Crick, C. R.; Bear, J. C.; Kafizas, A.; Parkin, I. P. *Adv. Mater.* **2012**, *24*, 3505−3508.
(19) Kamegawa, T.; Shimizu, Y.; Yamashita, H. *Adv. Mater.* **2012**, *24*, 3697−3700.
(20) Fujishima, A.; Honda, K. *Nature* **1972**, *238*, 37−38.
(21) Nakata, K.; Fujishima, A. *J. Photochem. Photobiol., C* **2012**, *13*, 169−189.
(22) Nakata, K.; Ochiai, T.; Murakami, T.; Fujishima, A. *Electrochim. Acta* **2012**, *84*, 103−111.
(23) Chong, M. N.; Jin, B.; Chow, C. W. K.; Saint, C. *Water Res.* **2010**, *44*, 2997−3027.
(24) Wang, Y.; Zhang, Y.; Zhao, G.; Tian, H.; Shi, H.; Zhou, T. *ACS Appl. Mater. Inter.* **2012**, *4*, 3965−3972.
(25) Chen, X. B.; Shen, S. H.; Guo, L. J.; Mao, S. S. *Chem. Rev.* **2010**, *110*, 6503−6570.
(26) An, T. C.; Chen, J. Y.; Nie, X.; Li, G. Y.; Zhang, H. M.; Liu, X. L.; Zhao, H. J. *ACS Appl. Mater. Interface* **2012**, *4*, 5988−5996.
(27) Enache, D. I.; Edwards, J. K.; Landon, P.; Solsona-Espriu, B.; Carley, A. F.; Herzing, A. A.; Watanabe, M.; Kiely, C. J.; Knight, D. W.; Hutchings, G. J. *Science* **2006**, *311*, 362−365.
(28) Law, M.; Greene, L. E.; ohnson, J. C.; Saykally, R.; Yang, P. D. *Nat. Mater.* **2005**, *4*, 455−459.
(29) Kim, H. N.; Moon, J. H. *ACS Appl. Mater. Interface* **2012**, *4*, 5821−5825.
(30) Lee, J. A.; Krogman, K. C.; Ma, M.; Hill, R. M.; Hammond, P. T.; Rutledge, G. C. *Adv. Mater.* **2009**, *21*, 1252−1256.
(31) Jiang, X.; Tian, X.; Gu, J.; Huang, D.; Yang, Y. *Appl. Surf. Sci.* **2011**, *257*, 8451−8456.
(32) Daouk, W. A.; Xin, J. H.; Zhang, Y. H. *Surf. Sci.* **2005**, *599*, 6569−6575.
(33) Abidi, N.; Cabrales, L.; Hequet, E. *ACS Appl. Mater. Interfaces* **2009**, *1*, 2141−2146.
(34) Montazer, M.; Pakdel, E.; Behzadnia, A. *J. Appl. Polym. Sci.* **2011**, *121*, 3407−3413.
(35) Deng, B.; Cai, R.; Yu, Y.; Jiang, H. Q.; Wang, C. L.; Li, J.; Li, L. F.; Yu, M.; Li, J. Y.; Xie, L. D.; Huang, Q.; Fan, C. H. *Adv. Mater.* **2010**, *22*, 5473−5477.
(36) Cai, R.; Deng, B.; Jiang, H. Q.; Yu, Y.; Yu, M.; Li, L. F.; Li, J. Y. *Radiat. Phys. Chem.* **2012**, *81*, 1354−1356.
(37) Hadjiivanov, K. I.; Klissurski, D. G. *Chem. Soc. Rev.* **1996**, *25*, 61−69.
(38) Xie, Y.; Heo, S. H.; Yoo, S. H. *Nanoscale Res. Lett.* **2010**, *5*, 603−607.
(39) Hubinger, S.; Nee, J. B. *J. Photochem. Photobiol., A* **1995**, *86*, 1−7.
(40) Miyauchi, M.; Nakajima, A.; Hashimoto, K.; Watanabe, T. *Adv. Mater.* **2000**, *12*, 1923−1927.
(41) Rathouský, J.; Kalousek, V.; Kolář, M.; Jirkovský, J.; Barták, P. *Catal. Today* **2011**, *161*, 202−208.
(42) Aarthi, T.; Narahan, P.; Madras, G. *J. Hazard. Mater.* **2007**, *149*, 725−734.
(43) Semsarilar, M.; Tom, J.; Ladmiral, V.; Perrier, S. *Polym. Chem.* **2012**, *3*, 3266−3275.
(44) Sivalingam, G.; Nagaveni, K.; Hegde, M. S.; Madras, G. *Appl. Catal., B* **2003**, *45*, 23−38.
(45) Tayade, R. J.; Natarajan, N. S.; Bajaj, H. C. *Ind. Eng. Chem. Res.* **2009**, *48*, 10262−10267.
(46) Carretero-Genevrier, A.; Boissiere, C.; Nicole, L.; Grosso, D. *J. Am. Chem. Soc.* **2012**, *134*, 10761−10764.